Typeset with jpsj2.cls <ver.1.0beta>

Theoretical Temperature-Pressure Phase Diagram for $\{N(CH_3)_4\}_2MnCl_4$

Daniil G. Sannikov, Grigorii A. Kessenikh and Hiroyuki Mashiyama[1]

Institute of Crystallography, Russian Academy of Sciences, Moscow 117333, Russia
[1] *Department of Physics, Faculty of Science, Yamaguchi University, Yamaguchi 753-8512*

(Received January 10, 2002)

Theoretical phase diagrams for $\{N(CH_3)_4\}_2MnCl_4$ are calculated by using a phenomenological approach. Expressions for thermodynamical potentials of different phases and for boundaries between these phases are given in an explicit or parametric form. The theoretical temperature-pressure phase diagrams are plotted. They show sufficiently well agreement with corresponding experimental diagrams.

KEYWORDS: phenomenological theory, T-P phase diagram, incommensurate, commensurate, TMATC-Mn compound

§1. Introduction

The crystal $\{N(CH_3)_4\}_2MnCl_4$ (TMATC-Mn) belongs to the large family of well studied tetramethylammonium tetrahalogenometalic compounds $\{N(CH_3)_4\}_2\,MX_4$, where M and X stand for divalent metals and halogens, respectively.[1–3] The theoretical approach to calculating the temperature-pressure (T-P) phase diagram for the crystals TMATC- M, specifically for TMATC-Zn, was worked out recently.[4]

This approach is based on the assumption that a special triple point, which was called the Lifshitz-type (LT) point, exists in the phase diagram. This point was theoretically introduced by Aslanyan and Levanyuk,[5] and it represents some similarity of the Lifshitz (L) point.[6] In the LT-point, as in the L-point, three lines of the phase transitions between the incommensurate (IC) phase, initial (C) phase and commensurate ($C_{0/1}$) phase, which is equitranslational with the C phase, are converged (see a classification and special features of such triple points[7]). Existence of the LT-point in the phase diagram is due to the distinctive features of dispersion of the soft optical branch of the normal vibration spectrum of the crystal responsible for the phase transitions. This branch in a certain range of parameters has two minima: one in the center of the Brillouin zone and the other in an arbitrary point of this zone.

The experimental T-P phase diagrams for TMATC-Mn are shown in Fig. 1,[8] and in Fig. 2 (in less range of T and P but in greater detail)[9] (see also diagrams reported by Hamaya *et al.*[10,11]). The aim of this paper is to construct theoretical phase diagrams for TMATC-Mn on the bases of the method developed previously.[4] First we construct the diagram on the plane of dimensionless coefficients D and A of the thermodynamic potentials (see below). Assuming the linear dependence of D and A on T and P, we then construct the T-P diagrams and compare them

with the experimental diagrams (Figs. 1 and 2).

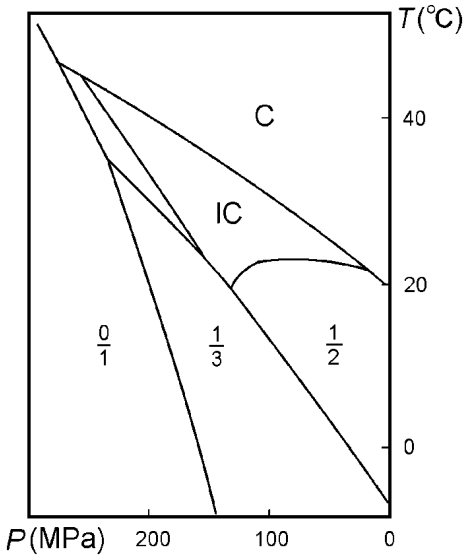

Fig. 1. The experimental T-P phase diagram for TMATC-Mn from Ref. 8. The notations of phases are the same as in Fig. 4.

The space group of the initial C phase is D_{2h}^{16} or $Pmcn$ (in bca setting which is usual for these crystals). The modulation vector of the IC phase is $k_z = qc^*$. The space groups of the $C_{m/l}$ phases with different wave numbers $q_{m/l} = m/l$ are the following: $q_{0/1}$ C_{2h}^5 $(P12_1/c1)$, $q_{1/3}$ C_{2h}^5 $(P112_1/n)$, $q_{2/5}$ C_{2v}^9 $(P2_1cn)$, $q_{3/7}$ D_2^4 $(P2_12_12_1)$ and $q_{1/2}$ C_{2h}^5 $(P2_1/c11)$ (see reports[1–3] and references therein). We assume, as indeed is the case, that all phases observed in TMATC-Mn are determined by the single optical branch of the normal vibration spectrum of the crystal (the language of lattice dynamics is useful for the case of displacive phase transitions as well as for order-disorder ones). The space groups of the $C_{m/l}$ phases are in agreement with this assumption. Table I of the previous report[4] gives the space groups for all possible $C_{m/l}$ phases corresponding to this branch (for details, see reference[12]).

§2. Thermodynamic Potentials

We use the expressions for thermodynamic potentials obtained previously,[4] adding the term proportional to ρ^6 (necessary, as can be seen from the following consideration). The potential of the $C_{m/l}$ phases (excluding the case of $q_{0/1} = 0/1$) has the form

$$\Phi_{m/l} = \alpha(q_{m/l})\rho^2 + \beta\rho^4 + \gamma\rho^6 - \alpha_l'\rho^{2l}\cos(2l\phi), \tag{1}$$

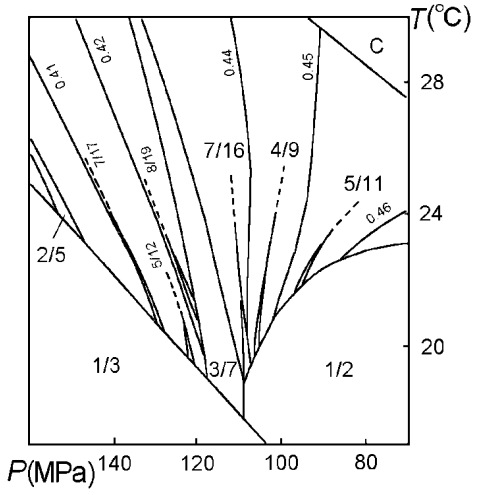

Fig. 2. The experimental T-P phase diagram for TMATC-Mn from Ref. 9.

where ρ and ϕ are the amplitude and phase of a two-component order parameter (the soft branch is doubly degenerate, i.e. $\alpha(q) = \alpha(-q)$). We assume $\beta > 0$ and $\gamma > 0$. The potential of the IC phase has the form

$$\Phi_{\rm IC} = \alpha(q)\rho^2 + \beta\rho^4 + \gamma\rho^6. \tag{2}$$

Note that the anisotropic term with the coefficient α_l' in Eq. (2) for an arbitrary incommensurate q does not satisfy a translational symmetry of the crystal and hence is not an invariant. The potential of the initial C phase and the commensurate $C_{0/1}$ phase has the form

$$\Phi_{0/1} = \alpha(q)\zeta^2 + \frac{2}{3}\beta\zeta^4 + \frac{2}{5}\gamma\zeta^6. \tag{3}$$

The soft optical branch, or more precisely, dependence of the elastic coefficient α on the wave number q, see Eqs. (1) and (2), is determined by the expression[5)]

$$\alpha(q) = \alpha - \delta q^2 - \kappa q^4 + \tau q^6, \tag{4}$$

where $\kappa > 0$ and $\tau > 0$ are assumed.

Eq. (4) can be rewritten in the form

$$\begin{aligned} &\alpha(q) = a + \Delta(q),\ \Delta(q) = \tau(b^2 - q^2)^2[2(b^2 - q_{\rm L}^2) + q^2],\ a = \alpha - \Delta_0, \\ &\Delta_0 = \Delta(0) = 2\tau b^4(b^2 - q_{\rm L}^2),\ \delta = \tau b^2(3b^2 - 4q_{\rm L}^2),\ q_{\rm L}^2 = \kappa/2\tau, \end{aligned} \tag{5}$$

where we introduce quantities a, b and $q_{\rm L}$ used in what follows. Their physical meaning is the following: a and b are coordinates of the minimum of the soft branch in an arbitrary point of the Brillouin zone:

$$q = b, \quad \alpha(b) = a. \tag{6}$$

This minimum exists at the values $\delta > -\kappa^2/3\tau$ or $b^2 > 2q_{\rm L}^2/3$. The minimum at the center of the Brillouin zone

$$q = 0, \quad \alpha(0) = \alpha \tag{7}$$

exists at the values $\delta < 0$ or $b^2 < 4q_{\rm L}^2/3$. Thus, in the interval of values $-\kappa^2/3\tau < \delta < 0$ or $2q_{\rm L}^2/3 < b^2 < 4q_{\rm L}^2/3$ the soft branch has two minima. The LT-point is determined by the condition that these minima simultaneously become zero. The coordinates of the LT-point, depending on the planes we use, are

$$a = 0,\ b = q_{\rm L},\ \delta = -\tau q_{\rm L}^4,\ \Delta_0 = 0. \tag{8}$$

Expressions (1)-(3) for the potentials can be simplified if we minimize them with respect to their variables. As a result we obtain, at $\gamma = 0$,[4)]

$$\begin{aligned} &\Phi_{\rm C} = 0,\ \Phi_{\rm IC} = -a^2/4\beta,\ \Phi_{0/1} = -3\alpha^2/8\beta, \\ &\Phi_{1/2} = -\alpha_{1/2}^2/4(\beta - \mid \alpha_2' \mid), \\ &\Phi_{m/l} = -\frac{\alpha_{m/l}^2}{4\beta}\{1 + \frac{\mid \alpha_l' \mid}{\beta}\left(-\frac{\alpha_{m/l}}{2\beta}\right)^{l-2}\}, \end{aligned} \tag{9}$$

where $\alpha_{m/l} = \alpha(q_{m/l})$. The last expression for $\Phi_{m/l}$ is obtained at the condition that the anisotropic (i.e. ϕ-dependent) invariant in Eq. (1) is small in comparison with the isotropic invariant[4)]

$$\frac{\mid \alpha_l' \mid \rho^{2l}}{2\beta\rho^4} = \frac{\mid \alpha_l' \mid}{2\beta}\left(-\frac{\alpha_{m/l}}{2\beta}\right)^{l-2} \ll 1. \tag{10}$$

We stress that neglecting the term $\gamma\rho^6$ in potentials (9) cannot be valid for $\Phi_{1/3}$. Indeed, if $\gamma = 0$ the minimum of $\Phi_{1/3}$, Eq. (1), at finite values of ρ^2 disappears very quickly as $\mid \alpha_{1/3} \mid$ grows, even at not too large values of $\mid \alpha_3' \mid$. (It occurs at $3(-\alpha_{1/3}) \mid \alpha_3' \mid /\beta^2 = 1$ or at $12A_3^2(A - D_{1/3}) = 1$ in notations of Eq. (13).) In order to avoid this, it is necessary to take into account the term $\gamma\rho^6$ and to suppose $\gamma \geq \mid \alpha_3' \mid$. Obviously, the term $\gamma\rho^6$ must be included in all potentials (not only in $\Phi_{1/3}$).

Minimizing Eqs. (1)-(3) with respect to their variables we now obtain more complicated than

in Eq. (9) equations for thermodynamic potentials

$$\begin{aligned}
\Phi_{\rm IC} &= -\frac{2\beta^3}{27\gamma^2}\{(1-\frac{3\gamma a}{\beta^2})^{3/2}-(1-\frac{9\gamma a}{2\beta^2})\},\\
\Phi_{0/1} &= -\frac{50}{27}\frac{2\beta^3}{27\gamma^2}\{(1-\frac{9}{10}\frac{3\gamma\alpha}{\beta^2})^{3/2}-(1-\frac{9}{10}\frac{9\gamma\alpha}{2\beta^2})\},\\
\Phi_{1/3} &= -\frac{2\beta^3}{27(\gamma-\mid\alpha_3'\mid)^2}\{[1-\frac{3(\gamma-\mid\alpha_3'\mid)\alpha_{1/3}}{\beta^2}]^{3/2}-[1-\frac{9(\gamma-\mid\alpha_3'\mid)\alpha_{1/3}}{2\beta^2}]\},\\
\Phi_{1/2} &= -\frac{2(\beta-\mid\alpha_2'\mid)^3}{27\gamma^2}\{[1-\frac{3\gamma\alpha_{1/2}}{(\beta-\mid\alpha_2'\mid)^2}]^{3/2}-[1-\frac{9\gamma\alpha_{1/2}}{2(\beta-\mid\alpha_2'\mid)^2}]\},\\
\Phi_{m/l} &= -\frac{2\beta^3}{27\gamma^2}\{(1-\frac{3\gamma\alpha_{m/l}}{\beta^2})^{3/2}-(1-\frac{9\gamma\alpha_{m/l}}{2\beta^2})\}-\mid\alpha_l'\mid\{\frac{\beta}{3\gamma}[(1-\frac{3\gamma\alpha_{m/l}}{\beta^2})^{1/2}-1]\}^l.
\end{aligned} \tag{11}$$

The last expression for $\Phi_{m/l}$ is obtained at the condition of weak anisotropy taking now the form

$$\frac{\mid\alpha_l'\mid}{2\beta}\{\frac{\beta}{3\gamma}[\left(1-\frac{3\gamma\alpha_{m/l}}{\beta^2}\right)^{1/2}-1]\}^{l-2}\ll 1, \tag{12}$$

which coincides with Eq. (10) if $3\gamma(-\alpha_{m/l})/\beta^2\ll 1$.

§3. Phase boundaries

Later on we use the following variables and parameters

$$\begin{aligned}
A=-\frac{a}{\tau Q^6},\ D_0=\frac{\Delta_0}{\tau Q^6},\ D_{m/l}=\frac{\Delta(q_{m/l})}{\tau Q^6},\ B=\frac{b}{Q},\ Q_{\rm L}=\frac{q_{\rm L}}{Q},\\
Q_{m/l}=\frac{q_{m/l}}{Q},\ D=\frac{\delta}{\tau Q^4},\ A_l=\frac{\tau Q^6}{2\beta}\left(\frac{\mid\alpha_l'\mid}{\tau Q^6}\right)^{1/(l-1)},\ A_\gamma=\frac{\tau Q^6}{2\beta}\left(\frac{\gamma}{\tau Q^6}\right)^{1/2}.
\end{aligned} \tag{13}$$

For convenience (see D-A diagram on Fig. 3) the sign of A is chosen opposite to that of a. Each $\mathrm{C}_{m/l}$ phase is characterized by only one dimensionless parameter A_l depending on the magnitude of the coefficient α_l'. There is one more parameter A_γ common for all phases. Since the coefficients α, δ, κ and τ are dimensionless by itself, Q is mere a number and we introduce it in Eq. (13) for the sake of choosing numerical values of different quantities when constructing the phase diagrams.

A phase diagram must be plotted on the plane of such two coefficients of the potentials, which are small, and hence their dependence on T and P is essential. The other coefficients are assumed to be independent of T and P which is justified because these coefficients are, generally speaking, not small. The small coefficients are δ and α and hence D and A. So we construct a phase diagram on the D-A plane, assuming that these variables linearly depend on T and P, while the rest quantities $Q_{\rm L}$, A_γ and A_l are supposed to be constant. Hence, constant are the coefficients κ, τ, β, γ and α_l'.

Equating potentials (12) to each other we obtain expressions for the boundaries between corresponding phases. We restrict ourselves by those which present on the experimental phase diagram.

The boundaries with the initial C phase: C-IC and C-$\mathrm{C}_{0/1}$ have, respectively, the form

$$A=0,\ A=D_0. \tag{14}$$

The boundaries IC-$C_{0/1}$, IC-$C_{1/3}$ and IC-$C_{1/2}$ have, respectively, the form

$$\begin{gathered}(1+12A_\gamma^2A)^{3/2}-(1+18A_\gamma^2A)=\\ \frac{50}{27}\{[(1+\frac{9}{10}12A_\gamma^2(A-D_0)]^{3/2}-[1+\frac{9}{10}18A_\gamma^2(A-D_0)]\},\\ \frac{1}{A_\gamma^4}\{(1+12A_\gamma^2A)^{3/2}-(1+18A_\gamma^2A)\}=\\ \frac{1}{(A_\gamma^2-A_3^2)^2}\{[1+12(A_\gamma^2-A_3^2)(A-D_{1/3})]^{3/2}-[1+18(A_\gamma^2-A_3^2)(A-D_{1/3})]\},\\ (1+12A_\gamma^2A)^{3/2}-(1+18A_\gamma^2A)=\\ (1-2A_2)^3\{[1+\frac{12A_\gamma^2(A-D_{1/2})}{(1-2A_2)^2}]^{3/2}-[1+\frac{18A_\gamma^2(A-D_{1/2})}{(1-2A_2)^2}]\}.\end{gathered}\tag{15}$$

Three boundaries C-IC, C-$C_{0/1}$, Eq. (14), and IC-$C_{0/1}$, Eq. (15) converge at a single point, which is the LT-point. Its coordinates on the D-A plane is

$$D=-Q_{\rm L}^4,\quad A=0,\tag{16}$$

(the values $B^2=Q_{\rm L}^2$ and $D_0=0$ correspond to this point, see Eq. (8)).

The boundaries $C_{0/1}$-$C_{1/3}$ and $C_{1/3}$-$C_{1/2}$ have, respectively, the form

$$\begin{gathered}\frac{50}{27}\frac{1}{A_\gamma^4}\{[1+\frac{9}{10}12A_\gamma^2(A-D_0)]^{3/2}-[1+\frac{9}{10}18A_\gamma^2(A-D_0)]\}=\\ \frac{1}{(A_\gamma^2-A_3^2)^2}\{[1+12(A_\gamma^2-A_3^2)(A-D_{1/3})]^{3/2}-[1+18(A_\gamma^2-A_3^2)(A-D_{1/3})]\},\\ \frac{1}{(A_\gamma^2-A_3^2)^2}\{[1+12(A_\gamma^2-A_3^2)(A-D_{1/3})]^{3/2}-[1+18(A_\gamma^2-A_3^2)(A-D_{1/3})]\}=\\ \frac{(1-2A_2)^3}{A_\gamma^4}\{[1+\frac{12A_\gamma^2(A-D_{1/2})}{(1-2A_2)^2}]^{3/2}-[1+\frac{18A_\gamma^2(A-D_{1/2})}{(1-2A_2)^2}]\}.\end{gathered}\tag{17}$$

The boundary IC-$C_{m/l}$, as it follows from Eqs. (11) and (12), has the form

$$A=\frac{D_{m/l}^{1/(l-1)}}{A_l}\left[1+\frac{3A_\gamma^2D_{m/l}^{1/(l-1)}}{A_l}\right].\tag{18}$$

This expression is obtained at the condition $D_{m/l}\ll A$, which coincides practically with the condition of weak anisotropy (12), which assumes in notations (13) the form

$$A_l\{\frac{A_l}{6A_\gamma^2}[(1+12A_\gamma^2A)^{1/2}-1]\}^{l-2}\ll 1.\tag{19}$$

For the $C_{m/l}$-$C_{m'/l'}$ boundary we obtain from Eq. (11) under the condition (19) the expression

$$\begin{gathered}D_{m/l}-\{\frac{A_l}{6A_\gamma^2}[(1+12A_\gamma^2A)^{1/2}-1]\}^{l-1}=\\ D_{m'/l'}-\{\frac{A_{l'}}{6A_\gamma^2}[(1+12A_\gamma^2A)^{1/2}-1]\}^{l'-1}.\end{gathered}\tag{20}$$

The boundaries $C_{m/l}$-$C_{1/3}$ and $C_{m/l}$-$C_{1/2}$ differ little from the boundaries IC-$C_{1/3}$ and IC-$C_{1/2}$, respectively, and these differences usually can be neglected (as it is done in Fig. 3).

The quantities $D_{m/l}$, D_0 and D are expressed in terms of B^2 according to Eq. (5) in the following way

$$\begin{aligned} D_{m/l} &= (B^2 - Q_{m/l}^2)^2[2(B^2 - Q_{\rm L}^2) + Q_{m/l}^2], \\ D_0 &= 2B^4(B^2 - Q_{\rm L}^2),\ D = B^2(3B^2 - 4Q_{\rm L}^2) \end{aligned} \tag{21}$$

Setting values of B^2 we can find values of A from Eqs. (14)-(20) and D from Eq. (21). This enables us to plot boundaries on the D-A diagram.

The minimum of the branch at an arbitrary point of the Brillouin zone disappears below the value $B^2 = \frac{2}{3}Q_{\rm L}^2$. Simultaneously the quantities a and b (A and B) lose their sense. Hence, the diagram on the D-A plane has the sense only at $D \geq -\frac{4}{3}Q_{\rm L}^4$.

§4. Theoretical Phase Diagrams

In order to construct the D-A phase diagram for TMATC-Mn we must chose values of the parameters $Q_{\rm L}$, A_γ, and A_l for each $C_{m/l}$ phase. Such choice is determined from the condition of best possible agreement between theoretical T-P diagrams, as obtained from the D-A diagram, and the experimental T-P diagrams shown in Fig. 1 and 2. We choose the following values of the parameters

$$Q_{\rm L}^2 = 0.55,\ Q = 0.5,\ A_2 = 0.375,\ A_\gamma = A_3 = 1,\ A_5 = 0.5,\ A_7 = 1.1. \tag{22}$$

They are taken with an accuracy only of one - two significant figures. The simplifying assumption $A_\gamma = A_3$ is used. Figure 3 shows the D-A phase diagram constructed according to expressions (14)-(21). LT denotes the LT-point with the coordinates given by Eq. (16). Note that there is no way of constructing the phase diagram on the D-A plane to the left of the dashed line (see also Fig. 4).

When constructing the T-P phase diagram from the D-A diagram given in Fig. 3, we assume the simplest linear dependence of D and A on T and P. Then the T and P axes are straight lines in Fig. 3. Their positions, orientations and scales are determined from the best possible agreement with the experimental T-P diagrams (Figs. 1 and 2). We put $\cot(\widehat{TD})$=0.3, $\cot(\widehat{PA})$=0.5.

Figures 4 and 5 shows the T-P phase diagram constructed from Fig. 3 with the choice of T and P axes indicated there. The scales along the T and P axes are chosen in the ratio of 0.7. By comparing Figs. 4 and 5 with Figs. 1 and 2, one can see that the theoretical and experimental phase diagrams agree sufficiently well. This agreement could be improved by making a more suitable selection of the parameters $Q_{\rm L}$, A_γ and A_l, and by achieving a more precise orientation of the T and P axes in the D-A diagram. A strong non-linearity of the dependencies of $q_{m/l}$ on T and P in

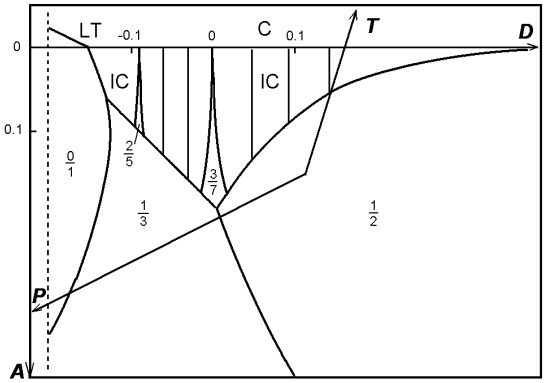

Fig. 3. The D-A phase diagram with the LT-point plotted for TAMTC-Mn.

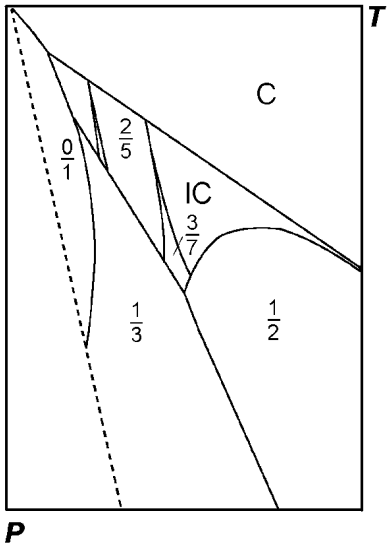

Fig. 4. The theoretical T-P phase diagram plotted on the bases of Fig. 3 for TMATC-Mn. The scale is the same as in Fig. 1.

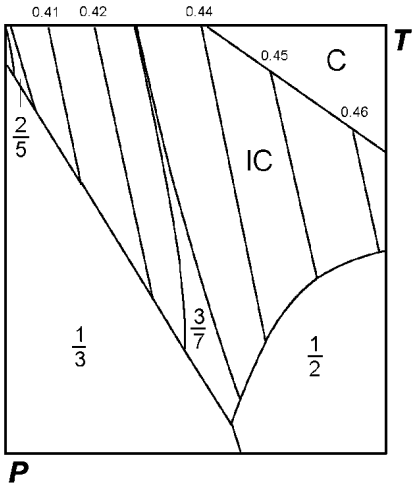

Fig. 5. The theoretical T-P phase diagram plotted on the bases of Fig. 3 for TMATC-Mn. The scale is the same as in Fig. 2.

Figs. 1 and 2 require to take into consideration nonlinear dependencies of A and D on T and P. But it is beyond the scope of this paper.

§5. Discussion

In conclusion, we enumerate again all approximations and assumptions made when constructing the theoretical D-A and T-P phase diagrams. The triple point between C, $C_{0/1}$ and IC phases existing in the experimental T-P diagrams for TMATC-M crystal family is assumed to be the LT-point[5] (and the L-point must be absent).

The single harmonic approximation is used for the IC phase. This leads to errors, although they are usually small when determining the boundaries between the IC and $C_{m/l}$ phases. The weak anisotropy condition is used for the $C_{m/l}$ phases ($m/l \neq 1/2$ and $1/3$). This allows us to obtain explicit expressions for the potentials and hence for the boundaries with the $C_{m/l}$ phases. This condition is comparatively well fulfilled in the whole region of the D-A and T-P phase diagrams in Figs. 3 and 4, 5.

Only two small quantities D and A are assumed to be dependent on T and P. The remaining quantities Q_{L}, A_γ and A_l (or κ, τ, β, γ and α_l') are considered to be constant, independent of T and P. The assumption of linear dependence of D and A on T and P is a simplification which obviously does not entirely quite correspond to the experimental diagrams (compare Figs. 1, 2 and 4, 5).

When constructing the phase diagrams the numerical values of the parameters are taken with, an accuracy of one - two significant figures. The simplification $A_\gamma = A_3$ is used. The dispersion (dependence on q) of the coefficients β, γ and α_l' is neglected.

The approximations and assumptions above-listed did not prevent us from obtaining a wholly satisfactory agreement between the theoretical and experimental T-P phase diagrams for TMATC-Mn. And this is in spite of the fact that in the phenomenological model considered here the number of dimensionless parameters which are used is small: $Q_{\rm L}$ determining the coordinate of the LT-point, A_γ, and A_l, which determines the width of the interval values q around $q_{m/l}$ occupying by the $C_{m/l}$ phases (at fixed values of A).

The phenomenological approach to structural phase transitions is known to be well justified. The present result shows that it is just as well justified in this case, i.e., as applied to complicated phase diagrams on which the special triple point of a new type, incommensurate phase, and a large number of commensurate phases exist. Thus this approach can be considered to be adequate to the experimental data.

Acknowledgements

Two of the authors (D.G.S. and G.A.K.) gratefully acknowledge the financial support of the Russian Fund of Fundamental Research (Grant No 02-00-17746).

---

1) J. D. Axe, M. Iizumi and G. Shirane: *Incommensurate Phases in Dielectrics 2*, ed. R. Blinc and A. P. Levanyuk (North-Holland, 1986, Amsterdam) Chap. 10.
2) K. Gesi: Ferroelectrics **66** (1986) 269.
3) H. Z. Cummins: Phys. Reports **185** (1990) 211.
4) D. G. Sannikov, G. A. Kessenikh and H. Mashiyama: J. Phys. Soc. Jpn. **69** (2000) 130.
5) T. A. Aslanyan and A. P. Levanyuk: Fiz. Tverd. Tela (Leningrad) **20** (1978) 804 [Sov. Phys. Solid State **20** (1978) 466.]
6) R. M. Hornreich, M. Luban and S. Strikman: Phys. Rev. Lett. **35** (1975) 1678.
7) D. G. Sannikov: Kristallogr. **41** (1996) 5. [Crystallography Reports **41** (1996) 1.]
8) K. Gesi and K. Ozawa: J. Phys. Soc. Jpn. **53** (1984) 627.
9) S. Shimomura, N. Hamaya and Y. Fujii: Phys. Rev. B **53** (1996) 8975.
10) N. Hamaya, Y. Fujii, S. Shimomura, Y. Kuroiwa, S. Sakaki and T. Matsusita: Solid State Commun. **67** (1988) 329.
11) N. Hamaya, S. Shimomura and Y. Fujii: J. Phys.: Condens. Matter **3** (1991) 3387.
12) D. G. Sannikov: Kristallogr. **36**, 813 (1991) [Sov. Phys. Crystallogr. **36** (1991) 455.]